External Dissipation in Driven Two-Dimensional Turbulence

Michael Rivera and X. L. Wu

Department of Physics and Astronomy, University of Pittsburgh, Pittsburgh, Pennsylvania 15260

(Received 20 September 1999)

Turbulence in a freely suspended soap film is created by electromagnetic forcing and measured by particle tracking. The velocity fluctuations are shown to be adequately described by the forced Navier-Stokes equation for an incompressible two-dimensional fluid with a linear drag term to model the frictional coupling to the surrounding air. Using this equation, the energy dissipation rates due to air friction and the film's internal viscosity are measured, as is the rate of energy injection from the electromagnetic forcing. Comparison of these rates demonstrates that the air friction is a significant energy dissipation mechanism in the system.

PACS numbers: 47.27.Jv

Laboratory fluids used for studying two-dimensional (2D) turbulence are not isolated. They interact with the three-dimensional (3D) environment which they are immersed in. This interaction is frictional and causes an energy leakage to the surroundings. For example, fluid motion in shallow layers is damped by the bottom of their containers [1,2]. Likewise, experiments in flowing soap films suffer from frictional coupling to the surrounding air [3–6]. Laboratory 2D turbulence thus has two energy dissipation mechanisms; energy can be dissipated by fluid's internal viscosity, or it can be bled to the environment by the frictional effect.

This frictional coupling is not restricted to laboratory fluids. Geostrophic flows are often modeled as 2D, and experience a similar coupling to the surface of the earth. In such flows, the coupling is modeled as a linear (or Rayleigh) drag term in the 2D Navier-Stokes equation:

$$\frac{\partial u_i}{\partial t} + u_s \frac{\partial u_i}{\partial x_s} = -\frac{1}{\rho}\frac{\partial p}{\partial x_i} + \nu \frac{\partial^2 u_i}{\partial x_s \partial x_s} + F_i - \alpha u_i , \tag{1}$$

where u_i is the ith component of velocity, p is the pressure, ρ and ν are the density and the kinematic viscosity of the fluid, F is the external force, and α is the Rayleigh drag coefficient. This description is appealing due to its simplicity; however, its validity to real fluid dynamic systems has not been quantitatively tested. The work reported here establishes that a Rayleigh drag model is adequate to describe the frictional force of air on a turbulent soap film that is maintained in a steady state by electromagnetic forcing. Such a soap film will be called an em cell.

Once Eq. (1) is established as consistent with data from the em cell, it can be used to estimate the rate at which air draws energy from the turbulence. It is also possible to measure the energy injection rate due to the em force and the energy dissipation rate due to the soap film's internal viscosity. Since the turbulence in the em cell is in the steady state, the energy dissipation rates must exactly balance the energy injection rate. Comparison of the dissipation rates gives a quantitative measure of the importance of air friction on turbulence in the em cell. Finally, the energy dissipation rates can be used to estimate the length scales at which dissipation takes place, and comment on energy and enstrophy flow characteristics of 2D turbulence.

A brief overview of the operation of the em cell is as follows. A film is drawn from a solution [400 ml water, 40 ml glycerol, 80 g ammonium chloride salt, 1% by volume liquid detergent (Joy), and a small amount of lycopodium (mushroom spores)] across an open square frame of area 7×7 cm^2. Two opposing sides of the square frame are made of stainless steel, and the remaining sides are plastic. A voltage difference is applied across the stainless steel sides to drive a current in the plane of the film. The voltage difference oscillates with a square waveform at 3 Hz. The film is then placed above an array of rare earth magnets which are oriented so that their magnetic field lines pierce the film perpendicularly. The turbulence which results is then measured by tracking the lycopodium particles. Two features of the experiment which deserve special attention are the magnet array and the measurement technique.

The spatial arrangement of the magnets below the film has profound effects on turbulence. It determines both the injection scale of turbulence as well as the efficiency of energy injection. In this experiment, the magnets are arranged such that the magnetic field varies approximately sinusoidally along the y axis and remains constant along the x axis. When an electric current is flowing across the film in the y direction, as shown in Fig. 1(a), a Lorentz force is generated which has approximately the following form: $F_x = F_0 \sin(k_y y)$ and $F_y = 0$, where $k_y \equiv 2\pi/a$ with $a = 0.6$ cm being twice the width of the magnets. That $\vec{F}$ is nondivergent, unidirectional, and translationally invariant along $\hat{x}$ will be exploited later in the analysis of our experimental data.

The velocity fields are measured with a particle tracking technique developed specifically for use in the em cell. It is similar in operation to particle imaging velocimetry (PIV) used earlier in soap films [5]. Lycopodium particles in the film are illuminated with a 12 mJ double-pulse Nd:YAG laser slaved to a CCD camera (8-bit, 768×480 rectangular pixels) so that corresponding

 0031-9007/00/85(5)/976(4)$15.00

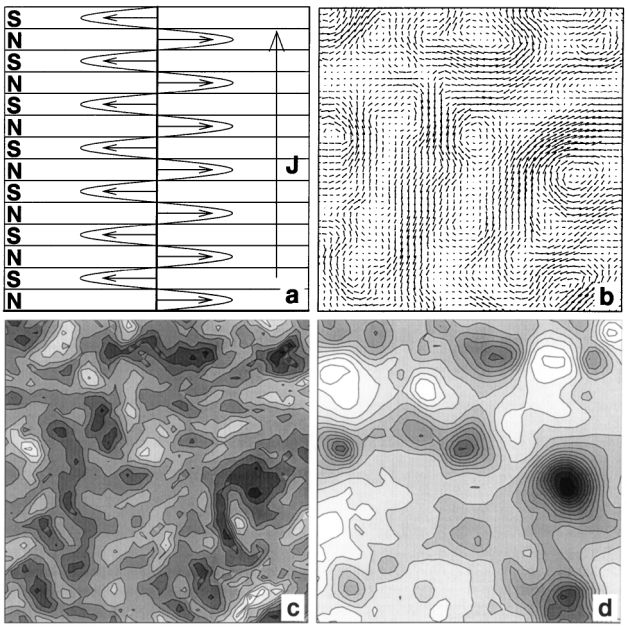

FIG. 1. (a) Top view of Kolmogorov magnets. The electric current is in the y direction, and the spatially periodic Lorentz force is in the x direction. A typical velocity, vorticity, and pressure field are displayed in (b), (c), and (d), respectively.

pulses straddle camera frames. By tracking individual particles instead of groups of particles, as in standard PIV, somewhat higher vector density can be achieved for the same raw images. However, unlike PIV, the vector fields generated by particle tracking are not snapped to a grid. This is not a drawback since the resultant vector fields can be interpolated to a grid with little sacrifice to large-scale velocity statistics.

Both the velocity field and the pressure field will be necessary to show that Eq. (1) adequately describes the fluid flow in the em cell. The reason for this will be made clear later. To obtain the pressure field $p(x, y)$, the divergence operator is applied to Eq. (1) and the fact that the force field is nondivergent is used to obtain

$$\rho^{-1} \frac{\partial^2}{\partial x_s \partial x_s} p = 2\Lambda, \tag{2}$$

where $\Lambda \equiv \frac{\partial u_x}{\partial x}\frac{\partial u_y}{\partial y} - \frac{\partial u_x}{\partial y}\frac{\partial u_y}{\partial x}$ [7]. Using Fourier techniques, $p(x, y)$ can be obtained for a given velocity field [8].

All data reported in this paper was extracted from a single run in the em cell with an applied voltage of 40 V and a current of 40 mA. Using these values and the resistivity of the bulk fluid, the film thickness, h, is $\sim 50\ \mu$m [9]. If one invokes the Trapeznikov [10] relationship between the film thickness and the viscosity, $\nu = \nu_b + 2\eta_s/\rho h$, a large h results in ν being close to that of the bulk fluid, $\nu_b = 0.01\ \text{cm}^2/\text{s}$. Recent measurements [11] of the surface viscosity of the surfactant layers, η_s, place its value at $\sim 1.5 \times 10^{-5}$ P · cm , thus yielding the film viscosity $\nu \sim 0.016\ \text{cm}^2/\text{s}$. The camera imaged a region of the fluid which was approximately $6 \times 4.5\ \text{cm}^2$, of which the central $4.5 \times 4.5\ \text{cm}^2$ section was used in the investigation. The laser flash spacing was 2 ms. Under these conditions, the film lasted approximately 30 min during which 1000 vector fields were extracted. Typical velocity, vorticity, and pressure fields from the run are shown in Figs. 1(b)–1(d).

Qualitative features of the turbulence are first measured to determine assumptions that can be made to simplify the data analysis. For each velocity field, the root-mean-square velocity $u_{\text{rms}}(t) \equiv [\frac{1}{A}\int_A d\vec{x}|\vec{u}(\vec{x}, t)|^2]^{1/2}$ and average enstrophy, $\Omega(t) \equiv \frac{1}{A}\int_A d\vec{x}[\omega(\vec{x}, t)]^2$, are calculated. Figure 2 shows that $u_{\text{rms}} \simeq 11 \pm 1$ cm/s and $\Omega = 3000 \pm 300\ \text{s}^{-2}$ throughout the lifetime of the film. It is also possible to calculate the mean-square divergence of the flow, $D(t) \equiv \frac{1}{A\Omega(t)}\int_A d\vec{x}[\vec{\nabla} \cdot \vec{u}(\vec{x}, t)]^2$, where $D(t)$ is normalized by $\Omega(t)$ so that it is nondimensional. By this definition $D(t)$ was found to be independent of time and $\sim 11\%$ of the enstrophy, which is consistent with an earlier measurement in thick soap films [5]. Alternatively, the compressibility of a fluid can be measured in terms of the Mach number, $M = u_{\text{rms}}/c$, where c is the speed of sound waves in the fluid. For our soap films, the relevant sound speed is the compressional wave which has $c \sim 200$ cm/s [12], giving $M \sim 0.06$ for the em cell. These estimates indicate that divergence in the system is small, and incompressibility may be assumed. The fact that u_{rms} is approximately constant in time also implies that the turbulence is in the steady state.

Directly demonstrating that Eq. (1) governs the time evolution of the turbulence in the em cell is difficult since it requires the measurement of a time derivative of a velocity field. At this time such a measurement is not possible. Instead, using the assumptions of homogeneity and incompressibility, Eq. (1) can be transformed to a time evolution equation for the two-point velocity correlation,

$$\frac{\partial}{\partial t}\langle u_i u_j' \rangle = \frac{\partial}{\partial r_s}[\langle u_i u_s u_j' \rangle - \langle u_i u_s' u_j' \rangle] - \frac{1}{\rho}\left[-\frac{\partial}{\partial r_i}\langle p u_j' \rangle + \frac{\partial}{\partial r_j}\langle p' u_i \rangle\right] + 2\nu \frac{\partial^2}{\partial r_s \partial r_s}\langle u_i u_j' \rangle + \langle u_i F_j' \rangle + \langle u_j' F_i \rangle - 2\alpha \langle u_i u_j' \rangle, \tag{3}$$

where u and u' denote the velocities at $\vec{x}$ and $\vec{x} + \vec{r}$, respectively, and $\langle \ldots \rangle$ is an ensemble average [13]. It should be emphasized that, due to unidirectional forcing, the pressure-velocity correlation in Eq. (3) cannot be ignored. This is in contrast to isotropic turbulence for which $\langle p u_i \rangle = 0$ [13]. Since the turbulence is in the steady state, the time derivative in Eq. (3) may be ignored. For large-scale velocity fluctuations, the viscous term in Eq. (3) is also small, resulting in

$$\frac{\partial}{\partial r_s}[\langle u_i u_s u_j'\rangle - \langle u_i u_s' u_j'\rangle] - \frac{1}{\rho}\left[-\frac{\partial}{\partial r_i}\langle p u_j'\rangle + \frac{\partial}{\partial r_j}\langle p' u_i\rangle\right] = -\langle u_i F_j'\rangle - \langle u_j' F_i\rangle + 2\alpha\langle u_i u_j'\rangle. \quad (4)$$

Determining that Eq. (4) is consistent with statistics from the em cell for $|\vec{r}|$ greater than some viscous-damping scale ($\ell_d \sim 250\ \mu$m) constitutes an indirect check that Eq. (1) is an appropriate equation for the dynamics in the em cell.

To simplify the measurements needed to test Eq. (4), we exploit the symmetries of the external force mentioned earlier. The fact that $\vec{F}$ is unidirectional, lying along the $\hat{x}$ direction, means that setting $(i, j) = (y, y)$ in Eq. (4) eliminates the forcing terms. The remaining terms are averaged over 1000 velocity fields, and the left-hand side and right-hand side of this equation [denoted by $L_{yy}(\vec{r})$ and $R_{yy}(\vec{r})$] are displayed for three different $\vec{r}$ cross sections in Figs. 3(a)–3(c). A least-square algorithm using α as the free parameter gives $\alpha \approx 0.7 \pm 0.3\ \mathrm{s}^{-1}$. Though the fit is noisy, $L_{yy}(\vec{r})$ and $R_{yy}(\vec{r})$ are definitely correlated. The noise may be due to a lack of convergence despite 1000 velocity fields used in the calculation. This is perhaps not surprising considering that the calculated $L_{yy}(\vec{r})$ contains derivatives of velocity triple correlations as well as velocity-pressure correlations. The fact that the data seems to contain small amplitude oscillations may be a reflection of residual inhomogeneity in the system, which was ignored in the analysis. Figure 3 leaves us with little doubt that the measurements are consistent with Eq. (4), showing that the Rayleigh drag term is adequate for modeling air friction on turbulent flowing soap films.

The energy dissipation rates due to viscosity and to air can now be determined. In the limit $r \to 0$, half the trace of Eq. (3) is given by

$$\frac{1}{2}\frac{\partial}{\partial t}\langle u_i u_i\rangle = -\epsilon_\nu + \epsilon_{\mathrm{inj}} - \epsilon_{\mathrm{air}}, \quad (5)$$

where $\epsilon_{\mathrm{inj}} = \langle F_i u_i\rangle$, $\epsilon_\nu = \nu\Omega$, and $\epsilon_{\mathrm{air}} = \alpha u_{\mathrm{rms}}^2$. The triple velocity correlation terms in Eq. (3) vanish in the single-point limit. Moreover, incompressibility combined with the trace operation eliminates the pressure terms. Using the above definitions of the energy dissipation rates, one finds $\epsilon_{\mathrm{air}} \simeq 85 \pm 35\ \mathrm{cm}^2/\mathrm{s}^3$ and $\epsilon_\nu \simeq 55 \pm 5\ \mathrm{cm}^2/\mathrm{s}^3$ for turbulence in the em cell. The system being in the steady state implies that $\epsilon_{\mathrm{inj}} (= \epsilon_\nu + \epsilon_{\mathrm{air}}) \simeq 140 \pm 40\ \mathrm{cm}^2/\mathrm{s}^3$.

To ascertain that the measured energy-rate constants are self-consistent, an independent measurement of ϵ_{inj} is necessary. This was done by exploiting Eq. (4) for $(i, j) = (x, x)$. In this equation the force-velocity terms do not vanish. However, since the force is invariant under a translation in the $\hat{x}$ direction, along the $r_y = 0$ cross section $\langle F_x' u_x\rangle = \langle F_x u_x\rangle = \langle F_x' u_x'\rangle = \langle F_x u_x'\rangle = \epsilon_{\mathrm{inj}}$.

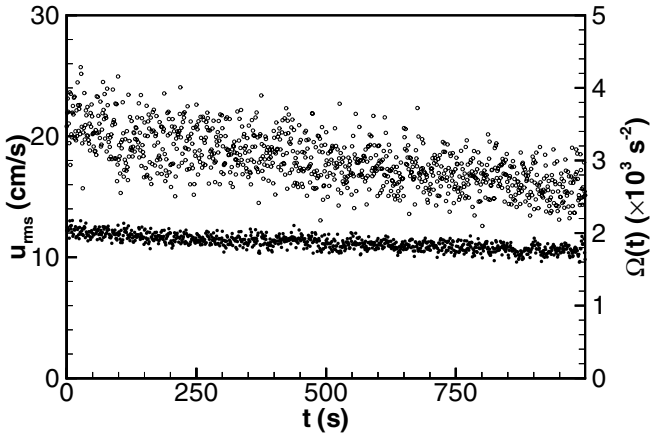

FIG. 2. The root-mean-square velocity $u_{\mathrm{rms}}(t)$ (•) and the enstrophy $\Omega(t)$ (∘) are plotted over a time span of 30 min.

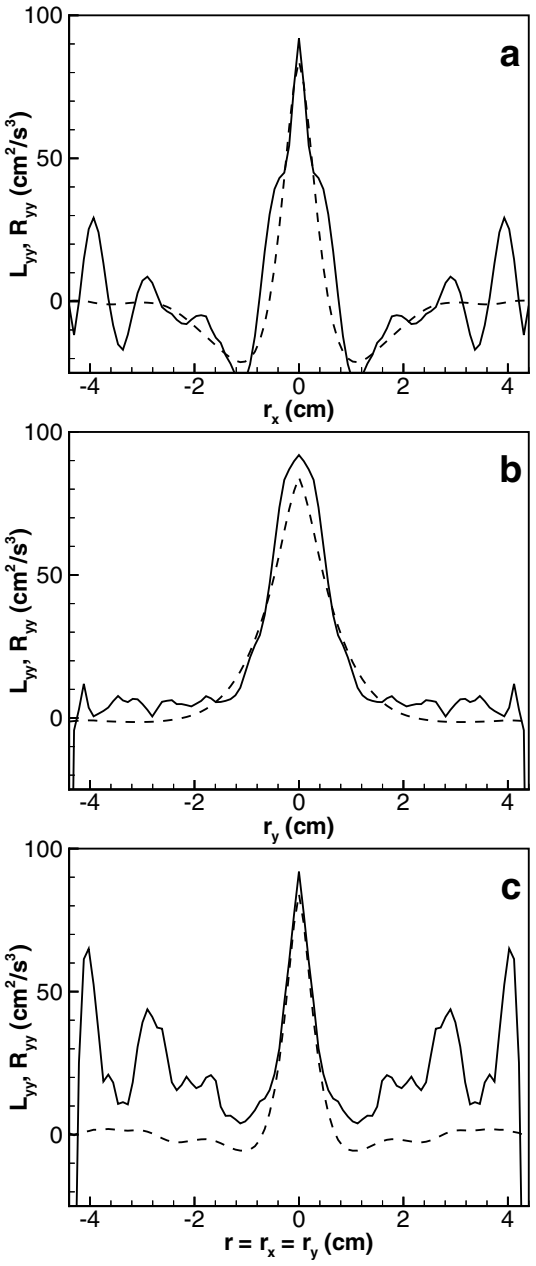

FIG. 3. $L_{yy}(\vec{r})$ (solid lines) and $R_{yy}(\vec{r})$ (dashed lines) for (a) $\vec{r} = (r_x, 0)$, (b) $\vec{r} = (0, r_y)$, and (c) $\vec{r} = (r_x, r_y)$ with $r_x = r_y$.

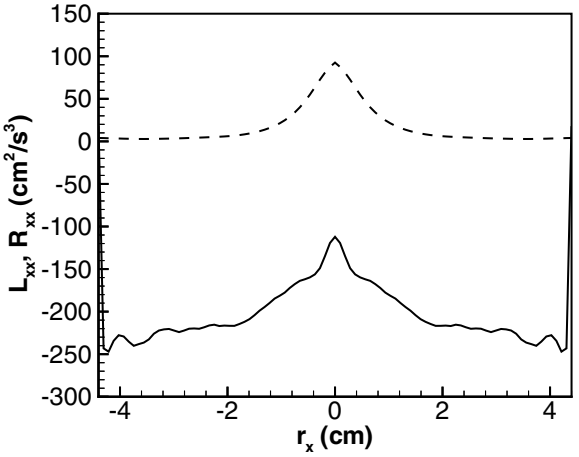

FIG. 4. $L_{xx}(\vec{r})$ (solid lines) and $R'_{xx}(\vec{r})$ (dashed lines) for $\vec{r} = (r_x, 0)$.

Figure 4 shows this cross section of $L_{xx}(\vec{r})$ and $R'_{xx}(\vec{r}) = R_{xx}(\vec{r}) + \langle u_x F'_x \rangle + \langle u'_x F_x \rangle = 2\alpha \langle u_x u'_x \rangle$. It is evident from this measurement that the R'_{xx} and L_{xx} essentially differ by a constant $2\epsilon_{\rm inj} \approx 240$ cm^2/s^3. To within experimental error, this independently measured $\epsilon_{\rm inj}$ agrees with that estimated using energy balance.

These energy rates can now be used to comment on enstrophy balance in the system. Since 2D turbulence contains no vortex stretching terms, the enstrophy also has a conservation equation in the steady state. This is given by

$$\beta_{\rm inj} - \beta_{\rm air} - \beta_\nu = 0 . \qquad (6)$$

Here, $\beta_{\rm inj}$ is the enstrophy injection rate which may be determined in our case by $k_y^2 \epsilon_{\rm inj} = \beta_{\rm inj}$, where $k_y = 2\pi/a$ is the injection wavelength. For $a = 0.6$ cm and $\epsilon_{\rm inj} \simeq 120$ cm^2/s^3, $\beta_{\rm inj} \simeq 1.2 \times 10^4$ s^{-3}. For the linear damping, $\beta_{\rm air} = \alpha\Omega = \frac{\alpha}{\nu}\epsilon_\nu \approx 2400$ s^{-3}. Enstrophy conservation therefore dictates $\beta_\nu \approx 10^4$ s^{-3}. It is clear that unlike energy, the enstrophy is predominantly dissipated by viscous forces.

Given the dissipation rates, various length scales in the em cell may be estimated. The largest length scales, or the outer scale ℓ_0, are determined by the balance between the advection term and the air-damping term in Eq. (1). The Reynolds number based on the Rayleigh drag may be defined as ${\rm Re}_{\rm air} \simeq u_{\rm rms}/\alpha\ell$, which when set equal to unity yields $\ell_0 \sim 15$ cm. This length scale is nearly twice the size of the em cell, so ℓ_0 cannot be directly measured in this experiment. It also implies that some finite energy dissipation may occur near the boundaries. The smallest length scale in the system, or the dissipation scale ℓ_d, is determined by $\ell_d \simeq \nu^{1/2}/\beta_\nu^{1/6}$, which as mentioned earlier is $\sim$250 μm.

These length scales allow for some speculation as to the directions of energy and enstrophy flow in the em cell. The current picture of 2D turbulence [14] has energy flowing from the injection scale ($a = 0.6$ cm) to larger scales. In contrast, enstrophy is predicted to flow from the injection scale to small scales. The data from the em cell supports this picture. The above dissipation rates suggest that energy is predominantly drained by air-film coupling. Since the typical length scale of the air friction is $\ell_0 \sim 15$ cm, much of this dissipation must be happening at scales larger than the injection scale $a = 0.6$ cm. Therefore a large portion of the energy must be advected by the turbulence from the injection scale to larger scales. A similar argument may be made to show the turbulence advects enstrophy to small scales.

With the magnitudes of the energy source and dissipation measured, it is clear that air is a non-negligible energy sink compared to the viscosity of the film and cannot be ignored. This is somewhat unsatisfying in that one normally expects an ideal fluid to have no damping other than the fluid's internal viscosity. On the other hand, the motion of energy to large scales in 2D demands that energy be taken out at some outer scales in order to establish a steady state. This work demonstrates that air plays such a role and can be adequately described by the Rayleigh drag term in the 2D Navier-Stokes equation. This finding allows 2D turbulence to be explored in a more quantitative fashion using the em cell.

We acknowledge helpful discussions with W. Goldburg and R. Cressman. This work was funded by NASA (NGT5-50207) and by the NSF (DMR-9731701).

[1] J. Sommeria, J. Fluid Mech. **170**, 139 (1986).
[2] J. Paret and P. Tabeling, Phys. Fluids **10**, 3126 (1998).
[3] M. Gharib and P. Derango, Physica (Amsterdam) **37D**, 406 (1989).
[4] H. Kellay, X. L. Wu, and W. I. Goldburg, Phys. Rev. Lett. **74**, 3975 (1995).
[5] M. Rivera, P. Vorobieff, and R. E. Ecke, Phys. Rev. Lett. **81**, 1417 (1998).
[6] J. M. Burgess, C. Bizon, W. D. McCormick, J. B. Swift, and H. L. Swinney, Phys. Rev. E **60**, 715 (1999).
[7] U. Frisch, *Turbulence: The Legacy of A.N. Kolmogorov* (Cambridge University Press, London, 1995).
[8] The pressure field is solved using a Fourier method assuming a periodic boundary condition. Strictly speaking, periodic boundary conditions are not satisfied in the em cell. It is expected that this has little influence on the pressure fields away from the boundaries.
[9] The menisci bordering the soap film can cause current leakage, and therefore affect the thickness measurements. However, such an effect was found to be small.
[10] A. A. Trapeznikov, in *Proceedings of the Second International Congress on Surface Activity* (Butterworths, London, 1957), p. 242.
[11] P. Vorobieff and R. E. Ecke, Phys. Rev. E **60**, 2953 (1999).
[12] Y. Couder, J. M. Chomaz, and M. Rabaud, Physica (Amsterdam) **37D**, 384 (1989).
[13] J. O. Hinze, *Turbulence* (McGraw-Hill, New York, 1975).
[14] R. Kraichnan, Phys. Fluids **10**, 1417 (1967).